reactions

MDPI

Article

Hydrolytic Oxidation of Cellobiose Using Catalysts Containing Noble Metals

Oleg Manaenkov [1,*], Olga Kislitsa [1], Ekaterina Ratkevich [1], Yuriy Kosivtsov [1], Valentin Sapunov [2] and Valentina Matveeva [1,3]

[1] Department of Biotechnology, Chemistry and Standardization, Tver State Technical University, 170026 Tver, Russia
[2] Department of Chemical Technology of Basic Organic and Petrochemical Synthesis, Mendeleev University of Chemical Technology, 125047 Moscow, Russia
[3] Regional Technology Center, Tver State University, 170100 Tver, Russia
* Correspondence: ovman@yandex.ru

Abstract: Studies of the processes of the hydrolytic oxidation of disaccharides are the first step towards the development of technologies for the direct conversion of plant polysaccharides, primarily cellulose, into aldonic and aldaric acids, which are widely used in chemical synthesis and various industries. In this study, heterogeneous catalysts based on a porous matrix of hypercrosslinked polystyrene (HPS) and noble metals (Pt, Au, Ru, and Pd) were proposed for the hydrolytic oxidation of cellobiose to gluconic and glucaric acids. The catalysts were characterized using low-temperature nitrogen adsorption, hydrogen chemisorption, electron microscopy, and other methods. In particular, it was shown that the Pt-containing catalyst contained, on average, six times more active centers on the surface, which made it more promising for use in this reaction. At a temperature of 145 °C, an O_2 pressure of 5 bars, and a substrate/catalyst weight ratio of 4/1, the yields of gluconic and glucaric acids reached 21.6 and 63.4%, respectively. Based on the data obtained, the mathematical model of the cellobiose hydrolytic oxidation kinetics in the presence of 3% Pt/HPS MN270 was developed, and the parameter estimation was carried out. The formal description of the kinetics of cellobiose hydrolytic oxidation was obtained.

Keywords: cellobiose; hydrolytic oxidation; glucaric acid; gluconic acid; noble metals; hypercrosslinked polystyrene

Citation: Manaenkov, O.; Kislitsa, O.; Ratkevich, E.; Kosivtsov, Y.; Sapunov, V.; Matveeva, V. Hydrolytic Oxidation of Cellobiose Using Catalysts Containing Noble Metals. *Reactions* **2022**, *3*, 589–601. https://doi.org/10.3390/reactions3040039

Academic Editors: Dmitry Yu. Murzin and József Sándor Pap

Received: 24 August 2022
Accepted: 11 November 2022
Published: 16 November 2022

1. Introduction

The products of glucose oxidation (gluconic and glucaric acids) are in-demand substances. In particular, gluconic acid is widely used in the food, pharmaceutical, metallurgical, and textile industries [1]. The demand for gluconic acid is constantly growing, and it is expected that by 2024, its consumption will reach 120 thousand tons per year [2]. Gluconic acid can be obtained via oxidation of glucose with chemical methods using heterogeneous catalysts, for example, based on gold nanoparticles [3], or with electrochemical methods associated with the use of electrodes made of noble metals [4]. However, the use of these methods in large-scale production is limited due to the harmful impact on the environment due to the high cost of catalysts, the likelihood of their deactivation, and the need for recycling or recovery [4]. More opportunities open up when enzymes are used [5,6]. However, the most promising is the production of gluconic acid with a biotechnological method [7,8], although some researchers also note the disadvantages of this option—a long fermentation process (15–24 h) and high operating costs [9].

Glucaric acid is a product of a deeper oxidation of glucose. Glucaric acid is also an important compound with wide prospects for use in various industries. According to the analytical portal Reports and Data [10], by 2027, the global market for glucaric acid will reach USD 1.46 billion. Back in 2004, the US Department of Energy included glucaric

acid in the list of substances with the highest added value that can be obtained from biomass and used in chemical synthesis [11]. In particular, it can be used for the production of detergents [12,13], polymers [14,15], and hydroxylated nylon [16]. Presently, glucaric acid is produced via the chemical oxidation of glucose, a nonselective, expensive, and environmentally unsafe process using nitric acid as an oxidizing agent [17]. Another option for the synthesis of glucaric acid is oxidation using heterogeneous catalysts. The reaction proceeds in two stages through the formation of gluconic acid. Literature data show that Pt- and Au-containing catalysts are very active in this process [18–20]. Promising results have been obtained through the electrocatalytic oxidation of glucose, which eliminates the use of high-pressure oxygen or other dangerous oxidizing agents and also makes it possible to control the selectivity of the process by adjusting the electrode potential [21–23].

A common disadvantage of the above methods for obtaining gluconic and glucaric acids is the use of mono- and disaccharides as feedstock, which can have nutritional value. From this point of view, plant biomass is an ideal raw material for the synthesis of aldonic and aldaric acids [24]. For example, in [25], a feasibility study was carried out for the production of pure glucaric acid from corn straw using two methods: the homogeneous oxidation of glucose with nitric acid and the oxidation of glucose with air in the presence of heterogeneous catalysts. The study showed that both options could be economically feasible for industrial applications—the costs per 1 kg of product were USD 2.91 and USD 2.53 for homogeneous and heterogeneous oxidation, respectively. However, the process using heterogeneous catalysts has a 22% lower environmental impact, with the main problem being the selection of a stable catalyst that is also characterized by a high yield of glucaric acid.

The promise of using the possibilities of heterogeneous catalysis for the synthesis of aldonic and aldaric acids from cellobiose is confirmed by the results of some works. For example, Morawa Eblagon et al. [26] used a 1 wt% Au/CX5.6 air citric catalyst for the conversion of cellobiose to gluconic acid with a selectivity of 80% (T = 418 K, 100 mL of 12 mM/L of cellobiose in water, 75 min, O_2 5 bar). It was shown that among the decisive factors determining the efficiency of the process are the adsorption properties and porosity of the support, which should be taken into account when developing multifunctional catalysts. In the study [27], a series of bimetallic catalysts, Au-M (M = Cu, Co, Ru, and Pd), based on TiO_2 were synthesized. The maximum selectivity for gluconic acid (88.5%) was obtained under the following conditions: cellobiose, 0.6 mmol; catalyst (Cu–Au/TiO_2), 0.100 g; H_2O, 20 mL; O_2, 1 MPa; 145 °C. On the basis of the obtained kinetic data, the authors proposed a reaction route. It was suggested that cellobiose is converted to cellobionic acid; then, gluconic acid is formed due to the cleavage of the β-1,4 glycosidic bond in cellobionic acid.

In this study, for the process of the hydrolytic oxidation of cellobiose to gluconic and glucaric acids, heterogeneous catalytic systems based on a polymer matrix of hypercrosslinked polystyrene (HPS) containing noble metals (Pt, Au, Ru, Pd) were proposed.

2. Materials and Methods

2.1. Materials

Hypersol-MacroNet without functional groups, designated as MN270 (Purolite Ltd., Llantrisant, UK) was utilized. D-(+)-cellobiose (>98%) was obtained from Carl Roth GmbH+Co. KG (Karlsruhe, Germany). Tetrahydrofuran (THF; ≥99.9%), methanol (MeOH; 99.5%), sodium hydroxide (NaOH; ≥98%), D-gluconic acid sodium salt (≥99%), D-saccharic (glucaric) acid potassium salt (≥98%), and D-(+)-Gluconic acid δ-lactone (≥99%) were obtained from Sigma-Aldrich (St. Louis, MO, USA). Ruthenium (IV) hydroxochloride, hydrogen hexachloroplatinate (IV) hydrate, sodium tetrachloropalladate (II) and gold (III) chloride hydrate (pure; OJSC Aurat, Moscow, Russia) were used as received. Distilled water was purified with an Elsi-Aqua water purification system.

2.2. Catalysts Synthesis

The synthesis of catalysts, in general, was carried out as follows: The granules of the original HPS MN270 were washed several times with hot (<40 °C) distilled water and acetone and were dried overnight at 50 °C. Dried HPS was crushed in a mill and separated into fractions using a vibrating sieve analyzer. For the synthesis of catalysts, a fraction of particles with a size of no more than 45 μm was used.

The dried polymer was impregnated according to moisture capacity with a solution of the calculated amount of noble metal precursor in a complex solvent consisting of tetrahydrofuran, methanol, and water at a volume ratio of 4:1:1 at room temperature. The use of a complex solvent is necessary for the most complete impregnation of HPS, which has a hydrophobic character. The catalysts were then dried at a temperature of 85 °C. The Ru-containing catalyst was additionally consecutively treated with hot (80 °C) solutions of NaOH and H_2O_2 to precipitate ruthenium oxide on the support surface and dried at 85 °C.

Then, the catalysts were reduced with hydrogen at 300 °C and an atmospheric pressure for 2 h, cooled in nitrogen, and kept under air.

Thus, using the appropriate precursors, 3% Me/HPS MN270 catalysts were synthesized (Me = Pt, Pd, Au, Ru).

2.3. Catalysts Characterization

Electron-transparent specimens for transmission electron microscopy (TEM) were prepared by placing a drop of a sample suspension onto a carbon-coated Cu grid. Images were acquired at an accelerating voltage of 80 kV on a JEOL JEM1010 transmission electron microscope (JEOL, Pleasanton, CA, USA). Images were analyzed with National Institute of Health-developed image-processing package ImageJ (NIH) to estimate nanoparticle diameters.

Liquid nitrogen physisorption was carried out using Beckman Coulter SA 3100 (Coulter Corporation, Miami, FL, USA). Prior to the analyses, each sample was placed in a quartz cell installed in Becman Coulter SA-PREP. Analyses were performed at −196 °C and at a relative pressure of 0.9814 (for pores less than 100 nm in diameter) to obtain a PSD (ADS) profile. The texture characteristics of the samples were calculated via the mathematical processing of nitrogen adsorption isotherms in accordance with the Brunauer–Emmett–Teller (BET), Langmuir, and de Boer–Lipens (t-plot) models.

The X-ray fluorescence analyses of the catalysts were performed on a VRA-30 analytical X-ray spectrometer (Zeiss, Jena, Germany).

The studies of the catalysts via H_2 chemisorption was carried out using a Chemosorb 4580 gas chemisorption analyzer (Micrometrics, Norcross, GA, USA).

The thermogravimetric analyses of the samples of hypercrosslinked polystyrene MN 270 were performed using a TG 209 IRIS thermogravimetric analyzer equipped with a DSC 204 PHOENIX differential scanning calorimeter (NETZSCH, Selb, Germany).

2.4. Catalyst Testing Procedure and Product Analysis

The experiments on the hydrolytic oxidation of cellobiose were carried out in a 50 cm^3 high-pressure steel reactor (Parr Instruments, Moline, IL, USA) with a PARR 4843 controller. In a typical test, the reactor was loaded with cellobiose, catalyst, and distilled water. After three times of purging the reactor with oxygen at a pressure of 5 bars, heating and stirring were switched on at a rate of ≈100 rpm to prevent the formation of local overheating zones. After reaching the operating temperature, the stirrer speed was increased to 600 rpm to transfer the reaction to the kinetic region. This moment served as the beginning of the countdown of the experiment. At the end of the experiment, the reactor was quickly cooled; the catalyst was separated using filtration through a paper filter; and the catalyzate was diluted to 50 cm^3 in a volumetric flask.

The analysis of the liquid phase of the catalyzate was carried out using the method of capillary zone electrophoresis under the following conditions: The background electrolyte was an aqueous solution of tryptophan (5 mM) and NaOH (50 mM); the analysis tem-

perature was 20 °C; the detector wavelength was 280 nm (indirect detection); the voltage was +20 kV; the inner diameter of the capillary was 50 μm; the capillary length up to the detector was 50 cm; hydrodynamic sample injection was conducted for 3 s at a pressure of 30 mbar. The analyses were carried out using a Kapel-105M capillary electrophoresis system (Lumex, St. Petersburg, Russia).

Cellobiose conversion was calculated using the following formula: $X = (n_{c0} - n_{cp})/n_{c0} \times 100\%$, where n_{c0} is the initial moles of cellobiose and n_{cp} is the moles of cellobiose in products. The product yield was calculated using the following formula: $\eta_p = n_p/n_{c0} \times k \times 100\%$, where n_p is the moles of product and k is the coefficient (for cellobionic acid, k = 1; for glucose, and gluconic and glucaric acids, k = 2). Product selectivity was calculated using the following formula: $S = n_p/n_c \times n_{pt} \times 100\%$, where n_c is the moles of cellobiose converted and n_{pt} is the theoretical number of moles of the product.

3. Results

3.1. Catalyst Characterization

The thermal stability of the polymer matrix of hypercrosslinked polystyrene was estimated using thermogravimetry. As it is shown in Figure 1, the intensive, multi-stage (probably, resulting from the break of the methylene cross links) destruction of HPS MN270 started at a temperature of about 450 °C (TG line). At this temperature, the polymer weight loss rate was maximum—10%/min (DTG line). The resulting weight loss was approximately 55%. These facts prove the possibility of the reduction of the catalyst on the basis of HPS MN270 with the gaseous hydrogen at a temperature 300 °C.

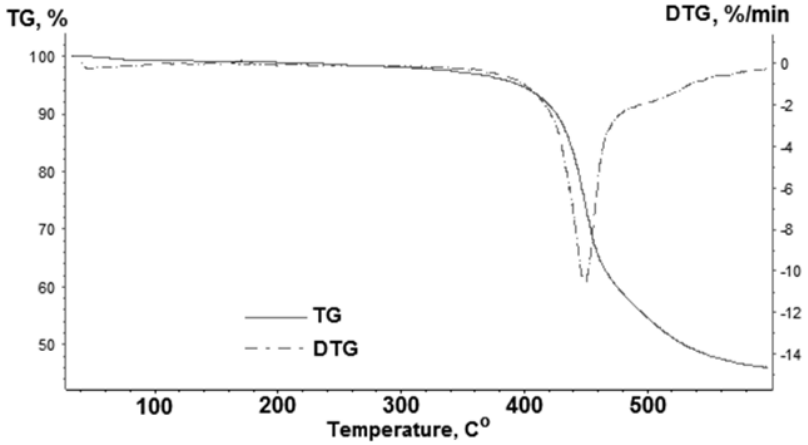

Figure 1. Results of thermogravimetric analysis of HPS MN270.

Table 1 presents the results of the X-ray fluorescence analyses of the synthesized catalysts. The elemental analysis data on the metal content had values close to the calculated values, which indicates the optimal nature of the used technique for the synthesis of catalytic systems based on HPS.

Table 1. Results of X-ray fluorescence analyses of the synthesized catalysts.

Catalyst	Me Loading, wt%	Me Content from Elemental Analysis, wt%
3% Pt/HPS MN270	3.00	2.91
3% Pd/HPS MN270	3.00	2.95
3% Au/HPS MN270	3.00	2.87
3% Ru/HPS MN270	3.00	2.70

Table 2 shows the values of the specific surface area of the sample of the HPS used in the work and the catalysts based on it. As can be seen from the data in the table, the samples had predominant microporosity with a highly developed internal surface. After

the introduction of metal nanoclusters into the composition of the polymer matrix, a change in its characteristics was observed; the specific surface area decreased due to the blockage of micro-, meso-, and macropores due to the formation of nanoparticles of the active phase of the catalyst. At the same time, the microporous nature of all samples was preserved.

Table 2. Results of the studies of the initial sample of HPS and the catalysts with the method of low-temperature nitrogen adsorption.

Sample	BET	Langmuir	t-Plot	
	S_{BET}, m^2/g	S_L, m^2/g	S_t, m^2/g	V, cm^3/g
HPS MN270	1075	1191	265 [1], 807 [2], 1072 [3]	0.37
3% Pt/HPS MN270	863	944	184 [1], 678 [2], 862 [3]	0.31
3% Pd/HPS MN270	649	758	94 [1], 553 [2], 647 [3]	0.22
3% Au/HPS MN270	738	810	141 [1], 593 [2], 734 [3]	0.25
3% Ru/HPS MN270	839	921	151 [1], 699 [2], 856 [3]	0.28

[1] Specific surface area surface of meso- and macropores. [2] Specific surface area of micropores. [3] Total specific surface area. S_L—specific surface area (Langmuir model); S_{BET}—specific surface area (BET model); S_t—specific surface area (t-plot); V—volume of micropores.

As a result of studying the synthesized catalysts with transmission electron microscopy (TEM), photographs and histograms of the size distribution of metal clusters were obtained (Figure 2). The average size of platinum nanoclusters was 2.8 nm; palladium, 3.4 nm; and ruthenium, 1.8 nm. The size of gold nanoclusters turned out to be approximately an order of magnitude larger, 32.1 nm, which apparently occurred due to the aggregation of nanoparticles during the synthesis of the catalyst. In general, it should be noted that the nanoparticles of all metals were uniformly distributed in the volume of the catalyst, and there was no metal crust on the polymer surface.

The study of the synthesized catalysts with the method of hydrogen chemisorption showed that the Pt-containing catalyst was characterized by a significantly larger number of active centers adsorbing hydrogen (Figure 3). Table 3 presents the quantitative results of the study. As can be seen from the data in Table 3, the concentration of active centers on the surface of 3% Pt/HPS MN270 exceeded similar indicators for other catalysts, on average, by six times. This fact can explain the higher activity of the Pt-containing catalyst in the reaction under study compared with catalysts containing other noble metals, as is shown below.

Table 3. Results of the studies of synthesized catalysts using H_2 chemisorption.

Sample	$c(H_2^{ads})$, $mmol(H_2)/g$
3% Pt/HPS MN 270	0.039
3% Pd/HPS MN 270	0.005
3% Ru/HPS MN 270	0.008
3% Au/HPS MN 270	0.005

3.2. Catalyst Testing

All synthesized catalysts were tested in the hydrolytic oxidation of cellobiose under the following conditions: cellobiose, 0.2 g; catalyst (3% Me/HPS MN270), 0.05 g; H_2O, 20 mL; 145 °C; O_2, 5 bar; reaction time, 1 h. The test results are shown in Table 4. The most active in the reaction was a Pt-containing catalyst, using which the cellobiose conversion was 100% and the yields of gluconic and glucaric acids were 16.1 and 41.5%, respectively. Such a high activity of the catalyst was most likely due to a much larger number of active sites on its surface compared with other catalysts.

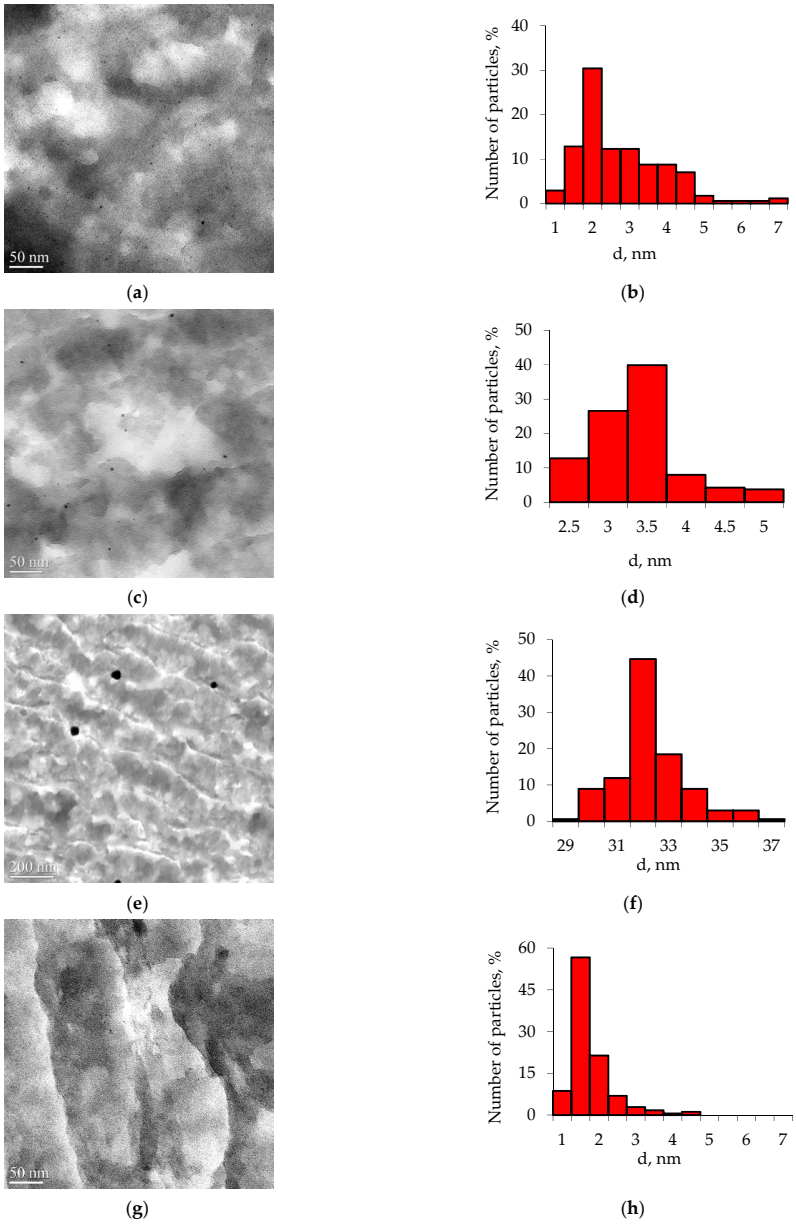

Figure 2. TEM images of catalyst samples and size distribution diagrams of metal-containing nanoparticles: (**a**,**b**) 3% Pt/HPS MN270; (**c**,**d**) 3% Pd/HPS MN270; (**e**,**f**) 3% Au/HPS MN270; (**g**,**h**) 3% Ru/HPS MN270.

Table 4. Cellobiose conversion and selectivity values of the main reaction products depending on the nature of the catalyst active phase metal.

Catalyst	Cellobiose Conversion, %	Product Selectivity, %				
		Glucose	Cellobionic Acid	Gluconic Acid	Glucaric Acid	Σ of By-Products
3% Pt/HPS MN270	100	4.1	9.4	16.1	41.5	28.9
3% Au/HPS MN270	86.2	24.6	50.1	12.3	0	13.0
3% Pd/HPS MN270	53.3	24.2	40.0	2.8	0	33
3% Ru/HPS MN270	45.4	26.4	0	0	0	73.6
blank (without catalyst)	9.5	14.7	0	0	0	85.3

Cellobiose, 0.2 g; catalyst, 0.05 g; H_2O, 20 mL; 145 °C; O_2, 5 bar; 1 h. By-products: acetic acid, succinic acid, oxalic acid, glycolic acid, glyceric acid, formic acid [26], and products of monosaccharide caramelization.

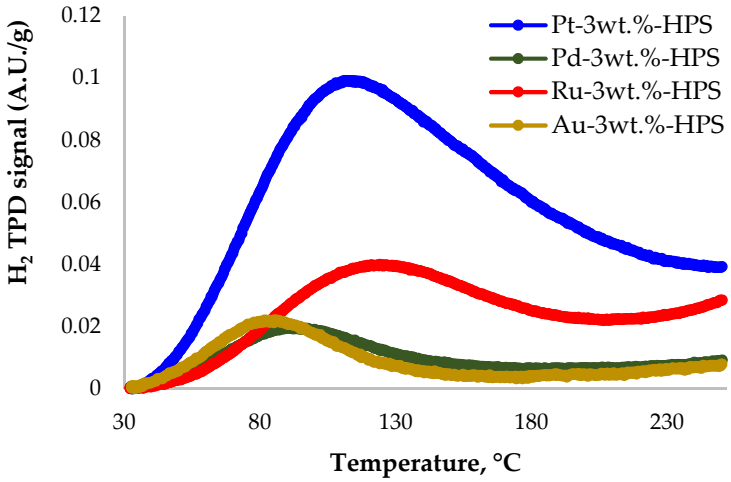

Figure 3. Results of thermogravimetric analyses of HPS MN 270.

The 3% Au/HPS MN270 catalyst proved to be less efficient in the oxidation reaction. After the end of the experiment, a sufficiently large amount of glucose (21.2%), cellobionic acid (43.2%), and an insignificant amount of gluconic acid (10.6%) were found in the catalyst. Glucaric acid was present in very small (trace) amounts. The conversion of cellobiose was 86.2%. The low activity of the Au-containing catalyst may have been due to the large particle size of the active phase. As shown in [26], some researchers believe that glucose oxidation is a structure-sensitive reaction and that for effective glucose oxidation, Au particles should be smaller than 5 nm. However, at the same time, the results of the study [26] showed that the sizes of Au nanoparticles do not play a decisive role in the hydrolytic oxidation of cellobiose.

Catalysts containing Pd and Ru showed the worst results, that is, a low conversion of the initial substrate and extremely low yields of gluconic and glucaric acids. The experiment without a catalyst showed that the catalyst plays the main role in the cellobiose hydrolysis reaction and that the degree of hydrolysis obviously depends on the nature of the metal that is part of the catalyst.

Therefore, further studies were carried out using the 3% Pt/HPS MN270 catalyst.

To optimize the temperature conditions of the reaction, the experiments were carried out in the range from 110 to 150 °C. The results obtained are shown in Figure 4. Optimum temperatures were determined to be between 140 and 150 °C. At these values, the conversion of cellobiose reached 100%, and the yields of gluconic and glucaric acids were maximum and practically did not increase with the increase in the temperature.

In the next stages of the study, the values of the reaction time and the substrate/catalyst ratio were optimized. Figure 5 shows the results of the final experiments.

As can be seen from the data in Figure 5, the maximum yield of gluconic acid (21.6%) corresponded to a reaction time of 1 h, and the maximum yield of glucaric acid (63.4%) was 2 h, with the other conditions being equal (145 °C; O_2, 5 bar; mass ratio substrate/catalyst, 4/1).

The stability of the 3% Pt/HPS MN270 catalyst was evaluated using it four times in the hydrolytic oxidation of cellobiose under the following conditions: cellobiose, 0.2 g; catalyst, 0.05 g; 145 °C, O_2, 5 bar, 2 h. The results are shown in Figure S1. It was shown that the conversion of cellobiose in all experiments was 100%, but the yields of gluconic and glucaric acids decreased by 5.5 and 11.0%, respectively. Presumably, the decrease in the yields of acids was due to the gradual degradation of the matrix of hypercrosslinked polystyrene as a result of polymer oxidation, as indicated by the obvious deterioration of its porous properties (Table S1). At the same time, the TEM results showed that the average size of Pt-containing particles of the spent catalyst remained almost unchanged, 2.9 nm (Figure S2a,b).

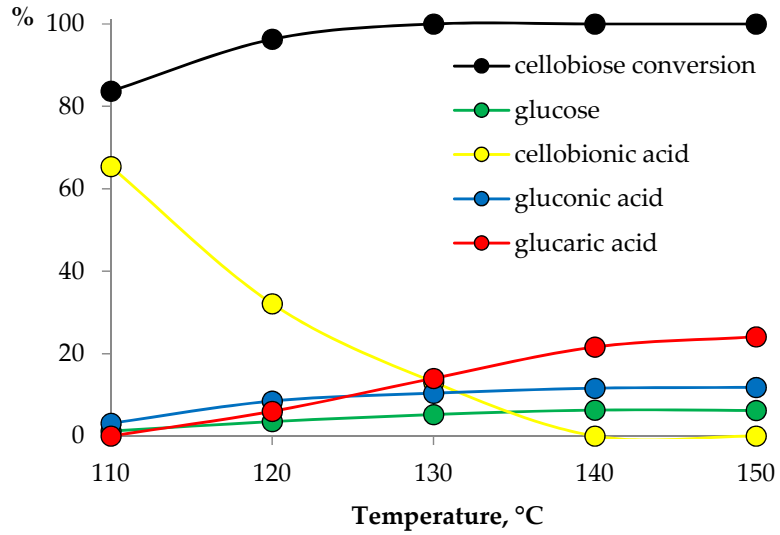

Figure 4. Dependence of cellobiose conversion and yields of main products according to the reaction temperature (cellobiose, 0.5 g; 3% Pt/HPS MN270, 0.1 g; H_2O, 20 mL; O_2, 5 bar; 3 h).

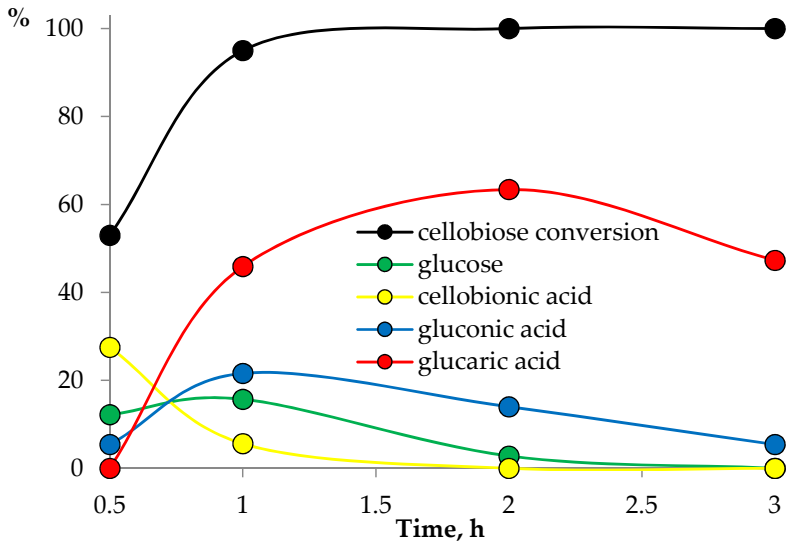

Figure 5. Dependence of the conversion of cellobiose and yields of the main products according to the reaction time (cellobiose, 0.2 g; 3% Pt/HPS MN270, 0.05 g; H_2O, 20 mL; 145 °C; O_2, 5 bar).

4. Discussion

In the process of optimizing the conditions for the hydrolytic oxidation of cellobiose, the obtained results of a qualitative and quantitative nature were analyzed. In particular, based on the temperature study data and the obtained electrophoregrams (Figure 6), a reaction scheme for the conversion of cellobiose to gluconic and glucaric acids in the presence of 3% Pt/HPS MN270 was suggested (Figure 7).

In the work of Armstrong et al. [28], it was shown that the oxidation of D-glucose using platinum catalysts to gluconic and glucaric acids proceeded with the formation of various lactones that were not determined using chromatographic methods. Obviously, in our study, the peaks of gluconic and glucaric acids on the electrophoregram corresponded to mixtures of these acids and their lactones, which we confirmed experimentally, in particular, in relation to gluconic acid and its lactone; in the model mixture, both substances appeared on the electrophoregram in one peak.

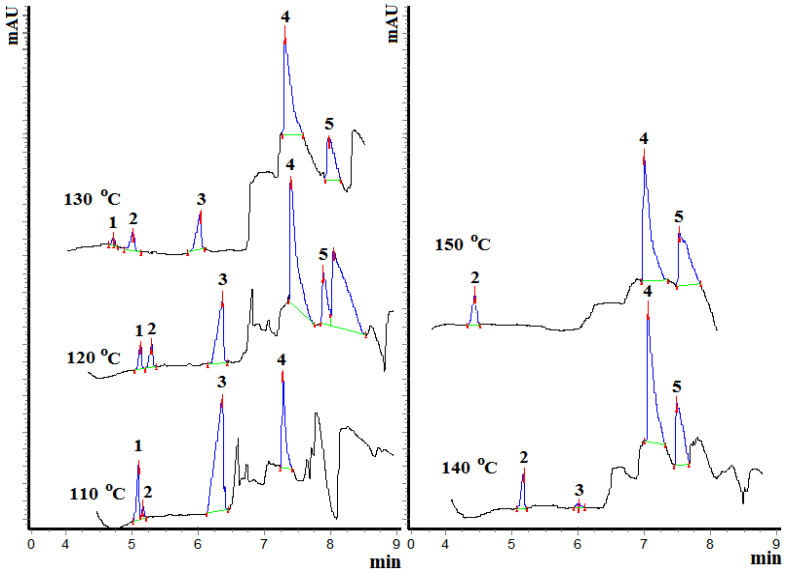

Figure 6. Electrophoregrams of the analysis of the catalyzate obtained at different reaction temperatures: 1—cellobiose; 2—glucose; 3—cellobionic acid; 4—gluconic acid; 5—glucaric acid (cellobiose, 0.5 g; 3% Pt/HPS MN270, 0.1 g; H_2O, 20 mL; O_2, 5 bar, 3 h).

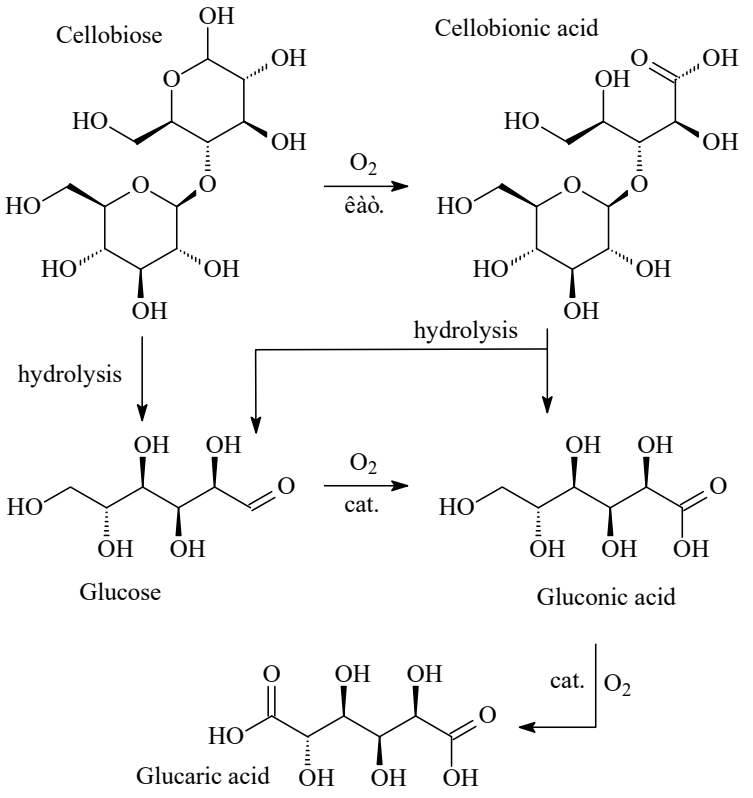

Figure 7. Proposed scheme for the conversion of cellobiose into gluconic and glucaric acids in the presence of a catalyst, 3% Pt/HPS MN270.

According to the data obtained, at a reaction temperature of 110 °C, the reaction mass mainly accumulated cellobionic acid (yield of up to 65%), which, similar to the initial cellobiose, further underwent hydrolysis, but with the formation of glucose and gluconic acid molecules. The conversion of cellobiose in this case was quite high and amounted to about 80%, and the yield of gluconic acid did not exceed 3.5%. Glucaric acid under such

conditions was determined in trace amounts. As the temperature rose, the rate of hydrolysis of cellobiose and cellobionic acid increased, and at 130 °C, the conversion of cellobiose reached 100%, while the yield of cellobionic acid decreased to 13%. At 140 °C, cellobionic acid was already present in the catalyzate in trace amounts. The acceleration of hydrolysis led to the accumulation of glucose in the reaction mass (up to 6%). It is characteristic that a noticeable increase in the yields of gluconic (from 8.7% to 12%) and, especially, glucaric (from 8.7% to 24%) acids was observed precisely in the range of 130–140 °C, when, with the accelerated decomposition of cellobionic acid, an additional amount of gluconic acid was rapidly oxidized at high temperatures to glucaric acid.

A further increase in the temperature led to the formation of brown solutions with a characteristic odor, which indicated the presence of glucose caramelization products in the catalyzate. In further experiments, the substrate/catalyst ratio was optimized to reduce the load on the catalytic system. The optimal mass ratio of cellobiose/3% Pt/HPS MN270 was 4/1. At these values, the resulting solutions were transparent, and there was no odor characteristic of glucose thermal degradation products.

The data obtained in this work were used for mathematical modeling, the essence of which was consistently described in our previous work [29]. As a result, a formal kinetic model of the process of cellobiose hydrolytic oxidation on the surface of the 3% Pt/HPS MN270 catalyst was constructed. To select an adequate kinetic model corresponding to the experimental data, various reaction pathways were analyzed, and the reaction scheme below was proposed (Figure 8).

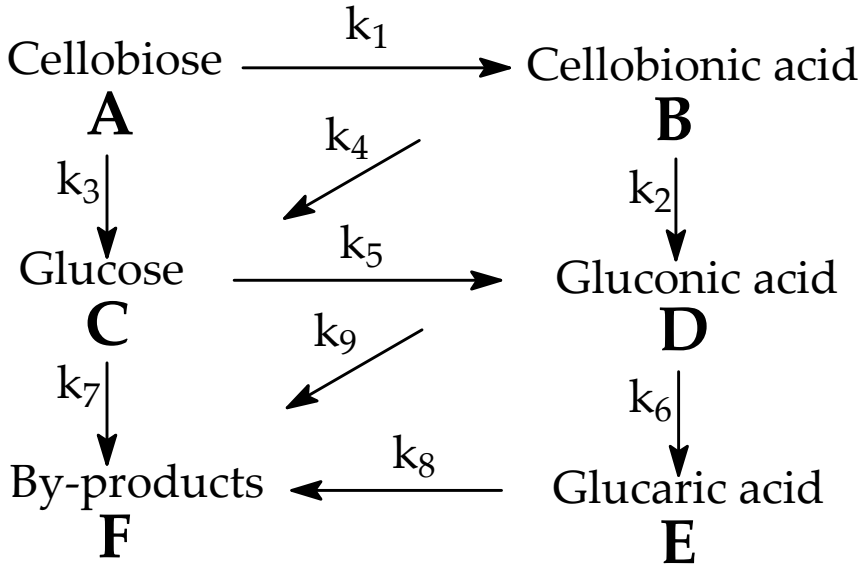

Figure 8. Scheme of the reaction of hydrolytic oxidation of cellobiose in the presence of the 3% Pt/HPS MN270 catalyst, obtained in the course of the mathematical modeling of the process.

For kinetic modeling, we used the reduced time parameter $\theta = \tau/q$, where τ is the reaction time and q is the load on the catalyst ($q = C_0/C_{cat}$, where C_0 is the substrate concentration and C_{cat} is the catalyst concentration). To generalize the experimental data obtained at different values of the load on the catalyst (q), a transition was made to the numerical concentration of cellobiose and its hydrolytic oxidation products in accordance with the formula $X_i = C_i/C_0$, where Ci is the current concentration of the product, mol/L, and C_0 is the current concentration of cellobiose, mol/L. The experimental data were reduced to coordinates X~θ. Thus, the mathematic modeling of the experimental data can be presented as a system of differential equations.

$$(dX_A/d\theta) = -k_1[A] - k_3[A] \quad (1)$$

$$(dX_B/d\theta) = k_1[A] - k_2[B] - k_4[B] \quad (2)$$

$$(dX_C/d\theta) = k_3[A] + k_4[B] - k_5[C] - k_7[C] \quad (3)$$

$$(dX_D/d\theta) = k_2[B] + k_5[C] - k_6[D] - k_9[D] \quad (4)$$

$$(dX_E/d\theta) = k_6[D] - k_8[E] \quad (5)$$

$$(dX_F/d\theta) = k_7[C] + k_8[E] + k_9[D] \quad (6)$$

where $(dX_i/d\theta)$—reaction rate at initial cellobiose concentration C_o = 1 mol/L and catalyst concentration $C_{cat.}$ = 1 mol/L.

The data calculated according to the model were compared with those obtained in the experiments. The value of the root mean square (RMS) deviation was used to choose the mathematic model fitting the experimental data (Figure 9).

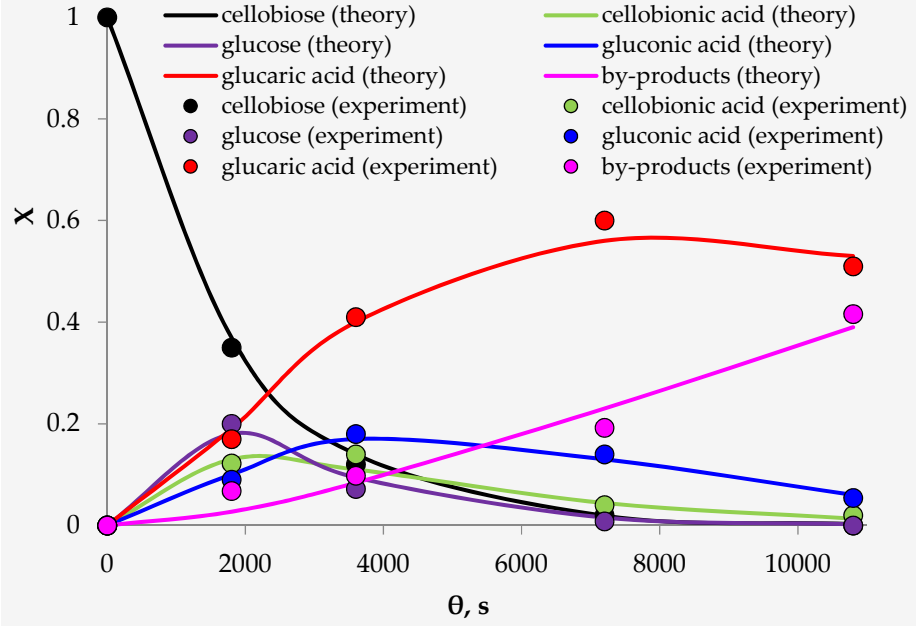

Figure 9. *X*~θ dependence for cellobiose hydrolytic oxidation using 3% Pt/HPS MN270.

The rate constant values calculated for cellobiose hydrolytic oxidation according to the model are presented in Table 5.

Table 5. Kinetic parameters obtained according to the mathematic model of cellobiose hydrolytic oxidation.

Parameter, $(mol/mol)_n \cdot s^{-1}$	Value	Parameter, $(mol/mol)_n \cdot s^{-1}$	Value
k_1	$2.49 \pm 0.07 \times 10^{-4}$	k_6	$4.99 \pm 0.15 \times 10^{-5}$
k_2	$5.96 \pm 0.18 \times 10^{-4}$	k_7	$2.18 \pm 0.06 \times 10^{-4}$
k_3	$2.88 \pm 0.09 \times 10^{-4}$	k_8	$3.82 \pm 0.11 \times 10^{-4}$
k_4	$4.56 \pm 0.14 \times 10^{-4}$	k_9	$7.34 \pm 0.22 \times 10^{-4}$
k_5	$5.97 \pm 0.18 \times 10^{-4}$		

RMS deviation of the experimental data from the calculated data: 4.10×10^{-2}.

The formal description obtained for the cellobiose hydrolytic oxidation using 3% Pt/HPS MN270 suggests the lack of adsorption or coordination interactions between the substrate or product molecules and the catalyst surface.

5. Conclusions

As a result of the study, an assessment was made of the possibility of using heterogeneous catalysts based on a polymer matrix of hypercrosslinked polystyrene containing noble metals (Pt, Pd, Au, Ru) in the hydrolytic oxidation of cellobiose to gluconic and glucaric acids. The use of Pt-containing catalytic systems in this reaction was shown to be promising. The optimal process conditions were determined as follows; at a temperature of 145 °C, an O_2 pressure of 5 bar, and a substrate/catalyst mass ratio of 4/1, the yields of gluconic and glucaric acids reached 21.6 and 63.4%, respectively, at 100% cellobiose conversion.

The formal description of the kinetics of cellobiose hydrolytic oxidation was obtained. The mathematic model of cellobiose conversion to gluconic and glucaric acids in the presence of 3% Pt/HPS MN270 was proposed. The kinetic parameter estimation was performed according to the model developed.

The results obtained can be further used to create a technology for the catalytic conversion of plant polysaccharides, primarily cellulose, into aldonic and aldaric acids, which are widely used in the chemical, food, pharmaceutical, and other industries.

Supplementary Materials: The following are available online at https://www.mdpi.com/article/10.3390/reactions3040039/s1, Figure S1. Cellobiose conversion and yield of main products upon repeated use of the catalyst (cellobiose 0.2 g; 3 % Pt/HPS MN270 0.05 g; H_2O 20 mL; 145 °C; O_2 5 bar, 2 h). Figure S2. TEM images of used 3 % Pt/HPS MN270 catalyst sample (a) and size distribution diagrams of Pt-containing nanoparticles (b). Table S1. The results of the study of the initial sample of the catalyst and the catalyst after four cycles of use.

Author Contributions: Conceptualization, O.M. and V.M.; methodology, Y.K. and V.S.; software, Y.K.; validation, O.K., and E.R.; formal analysis, E.R. and O.K.; investigation, O.M. and O.K.; resources, V.M.; data curation, Y.K.; writing—original draft preparation, O.M. and V.M.; writing—review and editing, O.M., V.M. and E.R.; visualization, O.K.; supervision, O.K.; project administration, V.M.; funding acquisition, V.M. All authors have read and agreed to the published version of the manuscript.

Funding: This research was funded by Russian Science Foundation, grant 22-79-10096.

Conflicts of Interest: The authors declare no conflict of interest.

References

1. Ramachandran, S.; Fontanille, P.; Pandey, A.; Larroche, C. Gluconic Acid: Properties, Applications and Microbial Production. *Food Technol. Biotechnol.* **2006**, *44*, 185–195.
2. Ahuja, K.; Singh, S. *Gluconic Acid Market by Application, by Downstream Potential, Regional Outlook, Application Potential, Price Trend, Competitive Market Share & Forecast, 2018–2024*; Global Market Insights Inc.: Selbyville, DE, USA, 2018; p. 240.
3. Biella, S.; Prati, L.; Rossi, M. Selective oxidation of D-glucose on gold catalyst. *J. Catal.* **2002**, *206*, 242–247. [CrossRef]
4. Pal, P.; Kumar, R.; Banerjee, S. Manufacture of Gluconic Acid: A Review towards Process Intensification for Green Production. *Chem. Eng. Process. Process Intensif.* **2016**, *104*, 160–171. [CrossRef]
5. Sulman, A.; Matveeva, V.; Golikova, E.; Grebennikova, O.; Lakina, N.; Doluda, V.; Karpenkov, A.Y.; Sulman, E. Oxidoreductase Immobilization on Magnetic Nanoparticles. *Chem. Eng. Trans.* **2019**, *74*, 487–492.
6. Neves, L.C.M.D.; Vitolo, M. Continuous production of gluconic acid and fructose using membrane bioreactor. *World J. Pharm. Pharm. Sci.* **2020**, *9*, 423–440.
7. Lim, H.Y.; Dolzhenko, A.V. Gluconic Acid Aqueous Solution: A BioBased Catalytic Medium for Organic Synthesis. *Sustain. Chem. Pharm.* **2021**, *21*, 100443. [CrossRef]
8. Ma, Y.; Li, B.; Zhang, X.; Wang, C.; Chen, W. Production of Gluconic Acid and Its Derivatives by Microbial Fermentation: Process Improvement Based on Integrated Routes. *Front. Bioeng. Biotechnol.* **2022**, *10*, 864787. [CrossRef]
9. Fernandes, S.; Belo, I.; Lopes, M. Highly Aerated Cultures Boost Gluconic Acid Production by the Yeast-like Fungus *Aureobasidium Pullulans*. *Biochem. Eng. J.* **2021**, *175*, 108133. [CrossRef]
10. Zhang, H.; Li, N.; Pan, X.; Wu, S.; Xie, J. Direct Transformation of Cellulose to Gluconic Acid in a Concentrated Iron(III) Chloride Solution under Mild Conditions. *ACS Sustain. Chem. Eng.* **2017**, *5*, 4066–4072. [CrossRef]
11. Reports and Data. Available online: https://www.globenewswire.com/news-release/2020/08/24/2082896/0/en/Glucaric-Acid-Market-To-Reach-USD-1-46-Billion-By-2027-Reports-and-Data.html (accessed on 10 July 2022).

12. Werpy, T.; Petersen, G.; Aden, A.; Bozell, J.; Holladay, J.; White, J.; Manheim, A.; Eliot, D.; Lasure, L. Top value added chemicals from biomass, volume 1—results of screening for potential candidates from sugars and synthesis gas. *Off. Sci. Tech. Inf.* **2004**, *69*, 36.
13. Grand View Research, Glucaric Acid Market Size, Share & Trends Analysis by Product (Pure Glucaric Acid, D-Glucaric Acid-1,4-Lactone), by Application (Food Ingredients, Detergents, Corrosion Inhibitors), & Segment Forecasts, 2017–2025. Available online: https://www.grandviewresearch.com/industry-analysis/glucaric-acid-market (accessed on 10 July 2022).
14. Wu, Y.; Enomoto-Rogers, Y.; Masaki, H.; Iwata, T. Synthesis of crystalline and amphiphilic polymers from d-glucaric acid. *ACS Sustain. Chem. Eng.* **2016**, *4*, 3812–3819. [CrossRef]
15. Mehtiö, T.; Toivari, M.; Wiebe, M.G.; Harlin, A.; Penttilä, M.; Koivula, A. Production and applications of carbohydrate-derived sugar acids as generic biobased chemicals. *Crit. Rev. Biotechnol.* **2016**, *36*, 904–916. [CrossRef] [PubMed]
16. Kiely, D.E.; Chen, L.; Lin, T.H. Hydroxylated Nylons Based on Unprotected Esterified D-Glucaric Acid by Simple Condensation-Reactions. *Am. Chem. Soc. Symp. Ser.* **1994**, *575*, 149–158. [CrossRef]
17. Smith, T.N.; Hash, K.; Davey, C.-L.; Mills, H.; Williams, H.; Kiely, D.E. Modifications in the nitric acid oxidation of d-glucose. *Carbohydr. Res.* **2012**, *350*, 6–13. [CrossRef] [PubMed]
18. Comotti, M.; Pina, C.D.; Rossi, M. Mono- and bimetallic catalysts for glucose oxidation. *J. Mol. Catal. A Chem.* **2006**, *251*, 89–92. [CrossRef]
19. Jin, X.; Zhao, M.; Shen, J.; Yan, W.; He, L.; Thapa, P.S.; Ren, S.; Subramaniam, B.; Chaudhari, R.V. Exceptional performance of bimetallic Pt_1Cu_3/TiO_2 nanocatalysts for oxidation of gluconic acid and glucose with O_2 to glucaric acid. *J. Catal.* **2015**, *330*, 323–329. [CrossRef]
20. Boussie, T.R.; Dias, E.L.; Fresco, Z.M.; Murphy, V.J. Production of Adipic Acid and Derivatives from Carbohydrate-Containing Materials. U.S. Patent 8501989B2, 11 June 2010.
21. Moggia, G.; Schalck, J.; Daems, N.; Breugelmans, T. Two-steps synthesis of D-glucaric acid via D-gluconic acid by electrocatalytic oxidation of D-glucose on gold electrode: Influence of operational parameters. *Electrochim. Acta* **2021**, *374*, 137852. [CrossRef]
22. Liu, W.; Xu, Z.; Zhao, D.; Pan, X.; Li, H.; Hu, X.; Fan, Z.; Wang, W.; Zhao, G.; Jin, S.; et al. Efficient electrochemical production of glucaric acid and H_2 via glucose electrolysis. *Nat. Commun.* **2020**, *11*, 265. [CrossRef]
23. Moggia, G.; Kenis, T.; Daems, N.; Breugelmans, T. Electrochemical oxidation of d-glucose in alkaline medium: Impact of oxidation potential and chemical side reactions on the selectivity to d-Gluconic and d-Glucaric Acid. *ChemElectroChem* **2020**, *7*, 86–95. [CrossRef]
24. Sakuta, R.; Nakamura, N. Production of Hexaric Acids from Biomass. *Int. J. Mol. Sci.* **2019**, *20*, 3660. [CrossRef]
25. Thaore, V.B.; Armstrong, R.D.; Hutchings, G.J.; Knight, D.W.; Chadwick, D.; Shah, N. Sustainable production of glucaric acid from corn stover via glucose oxidation: An assessment of homogeneous and heterogeneous catalytic oxidation production routes. *Chem. Eng. Res. Des.* **2020**, *153*, 337–349. [CrossRef]
26. Morawa Eblagon, K.; Pereira, M.F.R.; Figueiredo, J.L. One-pot oxidation of cellobiose to gluconic acid. Unprecedented high selectivity on bifunctional gold catalysts over mesoporous carbon by integrated texture and surface chemistry optimization. *Appl. Catal. B Environ.* **2016**, *184*, 381–396. [CrossRef]
27. Amaniampong, P.N.; Jia, X.; Wang, B.; Mushrif, S.H.; Borgna, A.; Yang, Y. Catalytic oxidation of cellobiose over TiO_2 supported gold-based bimetallic nanoparticles. *Catal. Sci. Technol.* **2015**, *5*, 2393–2405. [CrossRef]
28. Armstrong, R.D.; Hirayama, J.; Knight, D.W.; Hutchings, G.J. Quantitative Determination of Pt-Catalyzed D-Glucose Oxidation Products Using 2D NMR. *ACS Catal.* **2019**, *9*, 325–335. [CrossRef]
29. Manaenkov, O.; Kosivtsov, Y.; Sapunov, V.; Kislitsa, O.; Sulman, M.; Bykov, A.; Sidorov, A.; Matveeva, V. Kinetic Modeling for the "One-Pot" Hydrogenolysis of Cellulose to Glycols over $Ru@Fe_3O_4$/Polymer Catalyst. *Reactions* **2022**, *3*, 1–11. [CrossRef]